Check for updates

Received: 1 December 2020 | Revised: 16 March 2022 | Accepted: 23 March 2022

IET Renewable Power Generation

DOI: 10.1049/rpg2.12463

The Institution of Engineering and Technology WILEY

ORIGINAL RESEARCH

Blockchain based energy trading in ADN with its probable impact on aggregated load profile, available distribution capability and loadability margin

Devesh Shukla[1] | **Shailendra Singh**[1] | **Satyendra Pratap Singh**[2] | **Amit Kumar Thakur**[1] | **Shiv Pujan Singh**[1]

[1]Dept. of Electrical Engineering, IIT (BHU) Varanasi, Varanasi, India

[2]Dept. of Electrical Engineering, Arya College of Engineering & IT, Jaipur, Rajasthan, India

Correspondence
Devesh Shukla, Dept. of Electrical Engineering, IIT (BHU) Varanasi, Varanasi, India.
Email: deveshs.rs.eee15@itbhu.ac.in

Abstract

Power grids monitoring, operation, control, and commercialisation are transforming gradually due to technological advancements, and new frontiers of distinct applications are emerging in this field. Global emphasis on increasing the dependence on renewable sources of generation and the introduction of electric vehicles as means of transformation can potentially affect the traditional notion of grid analysis, monitoring, and control. The prevalence of communicable intelligent devices enables peers to transact and sell/buy power locally or to the grid. Ensuring security, privacy, and avoidance of double-spending in these transactions could be manifested by utilising the developments in blockchain technologies. In this paper, modified IEEE 123 bus distribution system has been considered. The effect of incorporating the energy transactions over block-chain in ADN on Available Distribution Capability, aggregated load profile, and load-ability is evaluated. The effect has been quantified using blockchain efficiency factor $\mathbf{BC_{ef}}$ proposed in this article. It has been observed that enabling intelligent electronic devices peers to transact over blockchain can improve the performance of the ADN.

1 | INTRODUCTION

Technological advancements brought forth various alterations and modifications to the conventional generation, transmission, and distribution methodologies. Emphasis on increasing the dependence on renewable sources of power generation at both the transmission and distribution levels transformed the intrinsically unidirectional power flow (from TN (transmission network) to DN (distribution network)) to bidirectional power flow [1]. Further, the shift in transportation modes from non-EV (electric vehicle) to EV-based systems added to the grids monitoring operation and control complexity. Under the ambit of these changing environments, intelligent electronic devices could participate in the power market and sell or purchase power to and from the grid using peer-to-peer networks. Blockchain-based technology provides a platform that could be used to deploy smart contracts through which the different players could transact.

In the era of wide-scale emphasis on renewable integration, the prosumers have ample opportunity to participate and reap the benefits of decentralised distributed generation through active participation in the energy markets. The prevalence of active sources DER's (distributed energy resources) and EVs as VPP (virtual power plant) would significantly impact the overall load profile of the *ADN* (Active Distribution Network) [2]. The inherent nature of renewable sources with uncertainty in generation in amalgamation with the complex behaviour of EV as VPP complicates the technological as well as commercial aspects of power system operation and control. The modelling of EVs and DER's have been done in refs. [2–6], where deterministic and probabilistic models have been proposed.

In literature, several articles have investigated the application of blockchain based systems for energy trading. [8–13]. Practical insight into designing a blockchain based energy trading platform has been discussed in ref. [10]. A taxonomy table showing the comparison of proposed work with a few recent articles

This is an open access article under the terms of the Creative Commons Attribution License, which permits use, distribution and reproduction in any medium, provided the original work is properly cited.
© 2022 The Authors. *IET Renewable Power Generation* published by John Wiley & Sons Ltd on behalf of The Institution of Engineering and Technology

TABLE 1 Taxonomy table showing the comparison of various articles

		ADN component considered						
			DER type					
S. N	Reference No	Prosumer	PV	WIND	EV	*μGrid*	Energy trading mechanism used	Platform used
1	[8]	Yes	No	No	No	No	Peer to peer energy trading; ADMM based mechanism	Blockchain
2	[17]	Yes	No	No	Yes	No	Peer to peer energy trading; Double Auction	Blockchain consortium
2	[9]	Yes	Yes	No	No	No	Peer to peer energy trading; double auction: game theoretic approach	Blockchain
3	[11, 14]	Yes	Yes	No	No	Yes	Peer to peer; proof of stake; double auction	Blockchain consortium
4	Proposed method	Yes	Yes	Yes	Yes	No	Peer to peer; double auction mechanism	Blockchain

has been shown in Table 1. In existing work, several methods have been proposed for deploying blockchain based energy trading in active distribution systems, but methods to quantify the effect of deploying blockchain based energy transaction in active distribution system still needs to evolve. In the present article, we have considered several components (Table 1) of ADN so as to analyse the impact of deploying blockchain based energy trading and ADN. Considering the blockchain-based energy trading in ADN, the impact on the overall aggregated load profile, available distribution capability, and load-ability of the system is assessed in this article. In the blockchain, distributed protocols are utilised for energy transactions between the load and generating nodes. Blockchain technology empowers the peers to transact digital value and information without the requirement of any third-party mediation; such features of blockchain are bound to enhance its applicability [14]. The probable changes in the modes of transformation to (EV/HEV (hybrid electric vehicles)) from conventional fuel-based systems would also necessitate the promulgation of blockchain technology for control and management of transactive energy [15].

A blockchain is a form of distributed ledger that offers immutability, security, and privacy. The double-spending problem encountered while exchanging the digital value could also be avoided using blockchain. Double spending refers to the phenomenon in which the same digital currency could be used for more than one purchase. Several techniques have been delineated in the literature that promulgates the deployment of blockchain-based methods for energy trade in the power sector. Blockchain-based distributed coalition formation for peer-to-peer energy trade among different microgrids has been presented in ref. [16]. Blockchain consortiums have been utilised to develop localised peer-to-peer electricity trading for plug-in-hybrid electric vehicles in smart grids [17]. A survey on blockchain from the perspective of game theory could be found in ref. [18]. Authors in ref. [19] have addressed the technical aspects concerned with the power flow constraints along with considering energy as a trading commodity and presented a block-chain model for managing ancillary services of microgrids.

The major contributions of this article are:

- A new index (BC_{ef}) have been proposed for quantising the effect of considering blockchain-based energy trading.
- The concept of localised marginal clearing price (LMCP) and localised marginal clearing volume (LMCV) for localised ADN under consideration have been proposed.
- The effect of considering the DER integration and blockchain-based energy trading on the load ability of the overall ADN under consideration is presented.
- The EV along with PV and DER have been considered as a component of ADN.

2 | TECHNO-ECONOMIC OPERATION OF ADN USING THE BLOCKCHAIN-BASED FRAMEWORK

The impact of changing technologies has been schematically illustrated in Figure 1 along with their features. Block-chain, preliminary introduced as a distributed ledger for recording and exchanging value by Satoshi Nakamoto [20].

Since then, applications of blockchain technology have arisen in varied dimensions. Block-chain comprises blocks that are nothing but a continuously growing list of data records. The blocks forming the blockchain are immutable, secure, and connected to the preceding block. Transactions can be initiated by any peer in the blockchain network. The blocks registering the transaction to the blockchain would be considered valid if it is accepted and approved by all the nodes in the network. The validation process for the blocks ensures their semantic and syntactic correctness. The transactions registered through the blocks on the blockchain could be accessed and verified by any node in the network. SHA256 [21] based hashing algorithm has been utilised for ensuring the security of each block. The hash of $(i-1)$th block is imbibed as an input to SHA256 function for obtaining the hash to subsequent block ith. Such a hashing system ensures that tempering at any one block creates invalid conditions among all the subsequent blocks in the chain. Consensus algorithm, along with the amalgam of the features

17521424, 2023, 11, Downloaded from https://ietresearch.onlinelibrary.wiley.com/doi/10.1049/rpg2.12463 by Indian Institute Of Technology, Wiley Online Library on [26/03/2024]. See the Terms and Conditions (https://onlinelibrary.wiley.com/terms-and-conditions) on Wiley Online Library for rules of use; OA articles are governed by the applicable Creative Commons License

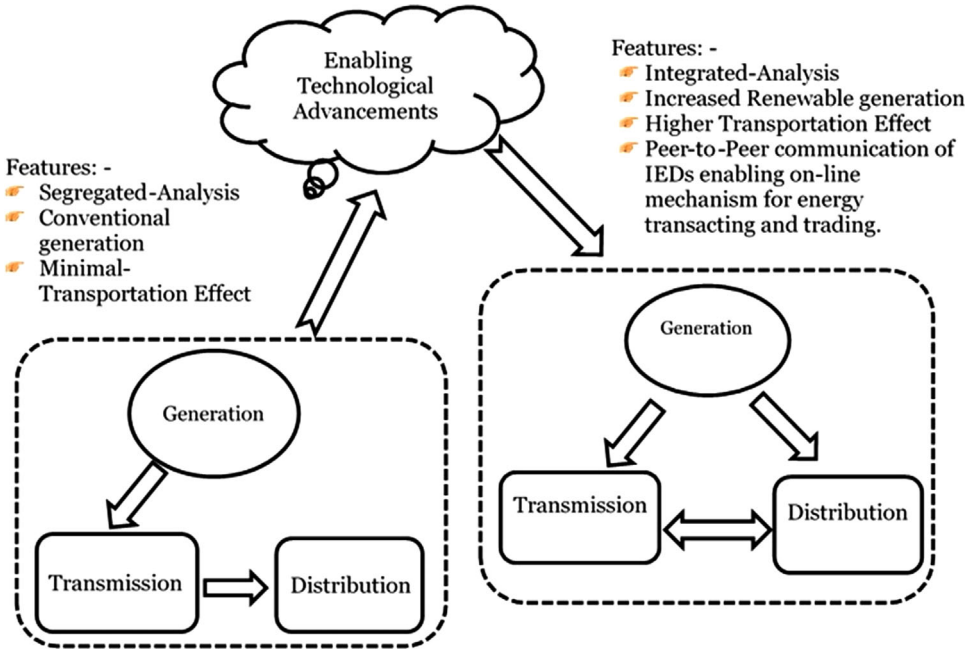

FIGURE 1 The changing technologies and its impact: schematic representation

mentioned above, protects the blockchain against colluding nodes with a certain degree of security and makes it highly resilient to tampering.

A schematic illustration of the proposed blockchain-based framework is given in Figure 2. The distributed coalition formation-based permission blockchain framework has been used. At each time instant, the information of actual power drawn/injected to the grid is communicated to the blockchain along with the bid for the impending instant. For each instance, the LMCP and LMCV are determined, and the information is sent to the DSO (distribution system optimiser). In DSO, the transactions are validated (the feasibility of each transaction is checked), and the settled price is updated and sent back to the blockchain network. The peer network of the ADN comprises the following auctioneers.

- Electric vehicle charging stations (EVCS) deployed at various nodes in the ADN.
- The distributed generators are presented in the ADN.
- The bids are submitted by the individual loads (considered as intelligent devices) through the local aggregators (LA).
- Transmission grid (selling or purchasing at the pcc. (point of common coupling) depending on the operating situations.)

The bid settlement process using the proportional sharing method has been discussed and given in ref. [2]. In the proportional sharing method, the total demand and losses of the ADN are proportionally shared among the bidding generators by the blockchain. In this article, LMCP and LMCV based methods have been proposed for determining the settlement price.

The procedure for LMCP and LMCV determination is given hereunder:

(i) LMCP determination

The LMCP determination has been proposed under the following assumptions:

a. The sellers and buyers participate in the bidding process through their bid functions $\mathcal{S}_i, \mathcal{B}_i$.
b. The sellers and buyers adhere to the following rules:
   i. The sellers and buyers will post their bids for the impending hour to the blockchain based transacting energy framework.
   ii. The sellers and buyers will post their actual consumption of the present hour to the blockchain-based transacting energy framework

Under these assumptions, a fair clearing price-based mechanism has been proposed here and utilised in this article for determining the LMCP and LMCV of the considered ADN. Let,

$$\mathcal{S}_i\ \left(Pg_{i,t}\right) = \alpha_i\ \mathcal{IC}_i \times Pg_{i,t} + \mathcal{OM}_i \times Pg_{i,t} \tag{1}$$

$$\mathcal{B}_i\left(Pd_{i,t}\right) = \beta_i Pd_{i,t}^2 + \psi Pd_{i,t} + \zeta_i \tag{2}$$

Here, α_i, is the cost of depreciation per unit, $\mathcal{IC}_i$ is installation cost per unit, $\mathcal{OM}_i$ operation and maintenance cost per unit of ith bidding DER unit at time instant t, β_i, ψ_i and ζ_i are the bid function coefficient of the ith bidding unit at time t. The sellers and buyers determine their impending hour production/demand using adequate forecasting techniques and use this for obtaining their bid price. These two values are posted to the blockchain-based framework. The process

17521424, 2023, 11, Downloaded from https://ietresearch.onlinelibrary.wiley.com/doi/10.1049/rpg2.12463 by Indian Institute Of Technology, Wiley Online Library on [26/03/2024]. See the Terms and Conditions (https://onlinelibrary.wiley.com/terms-and-conditions) on Wiley Online Library for rules of use; OA articles are governed by the applicable Creative Commons License

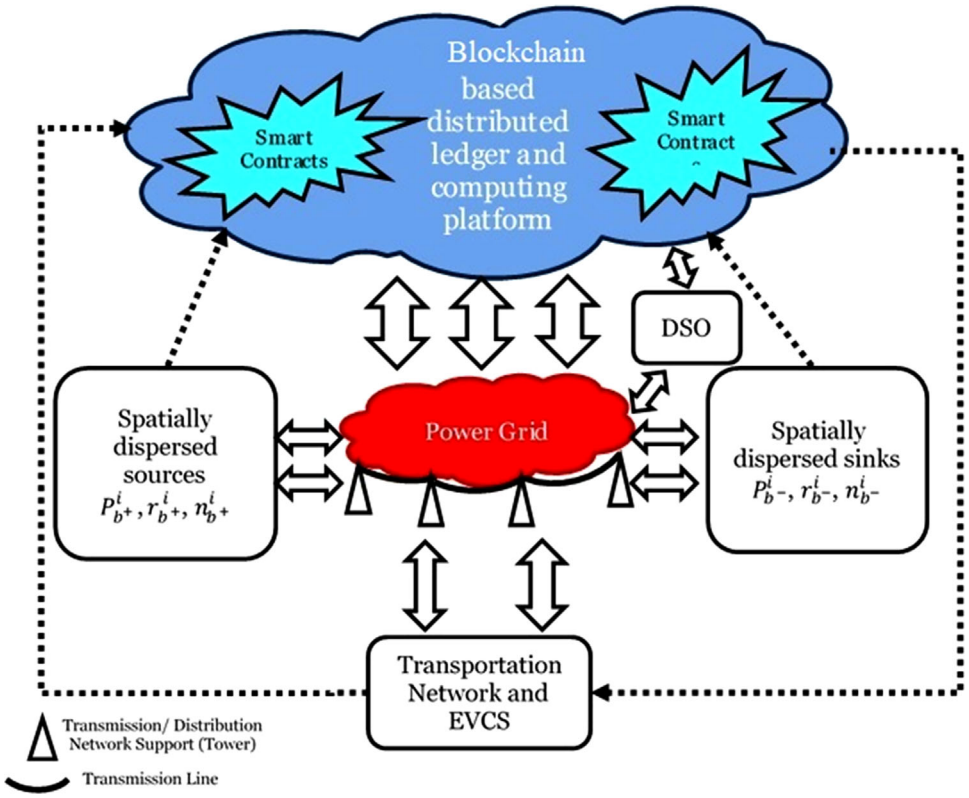

FIGURE 2 Schematic representation of blockchain implementation in ADN

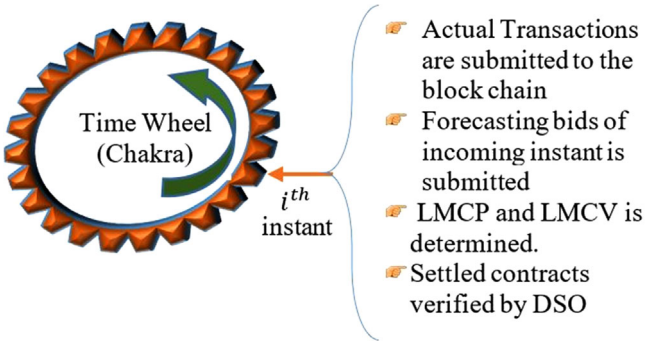

FIGURE 3 Sequential bid submission process on the blockchain

has been schematically illustrated in Figure 3. The steps of the LMCP and LMCV determination have been given in Table 2; the overall process has been shown in Figure 4.

(ii) DLMP determination

The distribution locational marginal pricing (DLMP) discussed in ref. [2] would be employed for the determination of DLMP by the DSO. The formulation would be adopted to the method proposed in this article by using LMCP price instead of LMP is illustrated in the following equations:

$$\text{DLM } P_i = \text{DLM}P_i^{\text{fixed}} + \text{DLM}P_i^{\text{loss}} \tag{3}$$

TABLE 2 Steps for obtaining the LMCP and LMCV

Steps	Algorithm
I	Acquire the bid prices from each local participant (including both buyers and seller, and Transmission grid bidding with LMP)
II	Arrange the sellers in the increasing order of their bids and buyers in the decreasing order of their bids.
III	Find the point of intersection of the two curves (seller bid curve and buyer bid curve).
IV	The point of intersection would yield the LMCP and LMCV, as illustrated in Figure 5.
V	If the grid is the seller and the LMCP determined is greater than the grid bid, i.e., LMP set the LMCP to LMP
VI	Post the LMCV and LMCP to the DSO for validation of the transaction.
VII	Evaluate the DLMP at node i at time t using Equations (3)–(5).

$$\text{DLM } P_i^{\text{fixed}} = \text{LMC } P_i^{\text{ADN}} = \lambda^{\hat{p}} \tag{4}$$

$$\text{DLM } P_{i,t}^{\text{loss}} = \lambda_t^{\hat{p}} + \sum_{i=1}^{f} \left(P(i,t)^{\{\text{loss}\}} \times \lambda_t^{\hat{p}} \right) \tag{5}$$

DLMP for different nodes is determined beforehand using the anticipated demand, generation, and weather scenarios. The actual energy transactions are

17521424, 2023, 11, Downloaded from https://ietresearch.onlinelibrary.wiley.com/doi/10.1049/rpg2.12463 by Indian Institute Of Technology, Wiley Online Library on [26/03/2024]. See the Terms and Conditions (https://onlinelibrary.wiley.com/terms-and-conditions) on Wiley Online Library for rules of use; OA articles are governed by the applicable Creative Commons License

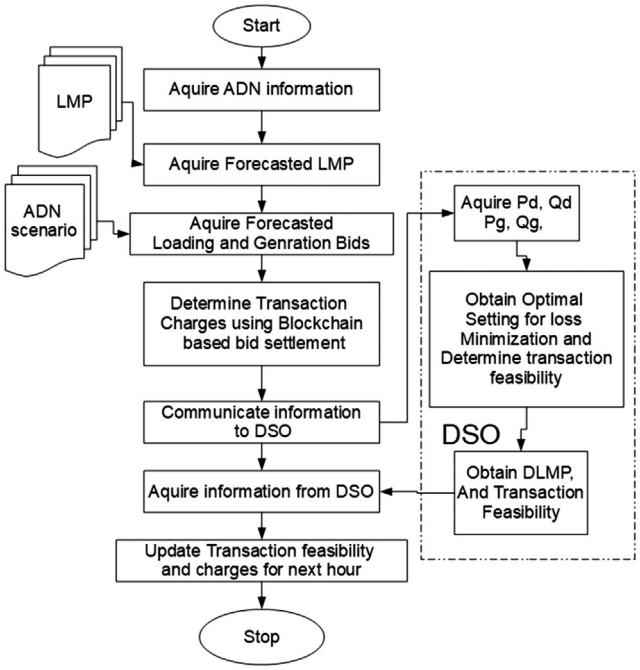

FIGURE 4 Flow chart for energy transaction scheduling and settlement process

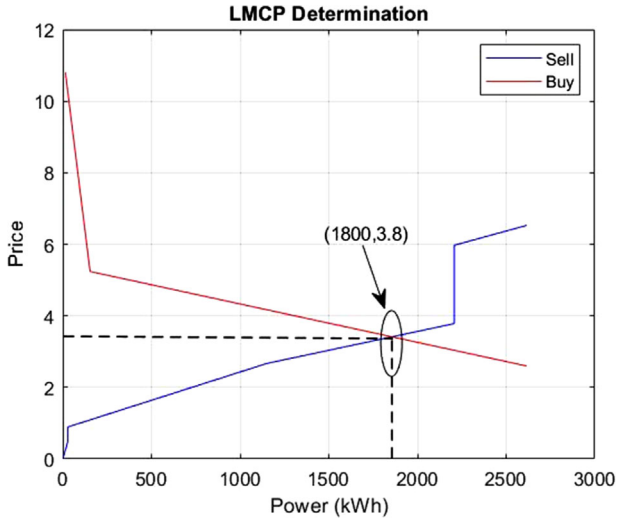

FIGURE 5 Illustration of LMCP determination

billed using estimated DLMP as pricing signals for various energy transactions taking place distinct players of the ADN.

3 | AVAILABLE DISTRIBUTION CAPABILITY, AGGREGATED LOAD PROFILE, AND LOADABILITY MARGIN

The net load profile subtended at the interface of transmission level by the ADN can be defined as the aggregated load profile (ALP). The ALP of the ADN would be depending on the participation of various energy vendors as well as active loads of ADN, and hence would have a probable impact of incorporating the energy transaction over the blockchain-based framework. Active load implies that the load would respond to price signals, provide bids for impending transactions, and send information pertaining to actual transactions to the blockchain through communicable intelligent devices. The total load profile represents the total load connected to the system; therefore, the ALP of an ADN would be different from its total load profile. ALP, in the simple sense, would be the total power injected/drawn at the TN interface. Thus, Aggregated Load of the ADN at time t would be obtained using Equation (6).

$$\mathcal{A}\,L_t = \sum_{i=1}^{ns} P_{i,t}^{\mathrm{PSS_{Trf}}} \tag{6}$$

In the above equation $P_{i,t}^{\mathrm{PSS_{Trf}}}$ is the subtended load at the ith source transformer of the ADN.

The maximum additional load that could be served by the generating entities to the nodes in the ADN while providing for the existing distribution commitments while satisfying the constraints of distribution has been defined as available distribution capability. Analogous to ATC (available transmission capability) at the transmission level, the available distribution capability (ADC) has been defined at the distribution level. ADC could be defined mathematically as Equation (7):

$$\mathrm{ADC} = \mathrm{TDC} - (\mathrm{EDC} + \mathrm{DRes}) \tag{7}$$

In the above equation, TDC, EDC, and DR are the total distribution capability (TDC), existing distribution commitments (EDC), and Distribution Reserves (DRes). DR has been provided so that the DG's could handle the weather uncertainties. The load-ability margin at any operating state of distribution system refers to the maximum load that can be served by the ADN under the allowable limits of voltage deviations while maintaining the other system constraints within limits.

$$\max\,(\mathcal{L}) \tag{8}$$

$$\textit{where},\ \mathcal{L} = \sum_{i} Pd_i \tag{9}$$

The optimisation given above is solved while adhering to the impediments of the distribution power flow.

4 | ADN COMPONENT MODELING

4.1 | Electric vehicles and their charging

The complete psychological and techno-economic behaviour pertaining to EV operation are modelled using an agent-based approach. In Table 3, the taxonomy of the EV structure has

17521424, 2023, 11, Downloaded from https://ietresearch.onlinelibrary.wiley.com/doi/10.1049/rpg2.12463 by Indian Institute Of Technology, Wiley Online Library on [26/03/2024]. See the Terms and Conditions (https://onlinelibrary.wiley.com/terms-and-conditions) on Wiley Online Library for rules of use; OA articles are governed by the applicable Creative Commons License

TABLE 3 EVagent taxonomy

EVagent	Field	Detail
	SoC	State of charge
	t	Time
	V_{id}	Vehicle id
	loc	Location of the EV
	EV_{av}	Availability of EV
	Tstopa	Estimated stopping time if vehicle is running
	Tstarta	Time at which the trip started
	EV_{Prob}	Probability of connecting to grid for charging/discharging.
	Dmax	Maximum estimated distance that EV can travel based on current SoC
	D	Distance travelled in current trip.
	c_{stat}	Charging status
	Te	Time elapsed from the start of current ride.
	Tr	Estimated time remaining in current ride.
	EV_{Speed}	Speed of the vehicle.
	Cs_d	Array vector containing the distance information from the nearest charging station.
	C_{db}	Array containing information of charging station accepting the request of allowing the vehicle to charge.
	CS_{name}	Charging station name/id
	C_r	Charging/discharging rate at which vehicle is feeding or absorbing power from–to grid
	Tcs	Time at which the vehicle is connected to the charging station

TABLE 4 Structure field and their details for charging station (CSAgent)

CSAgent	Field	Detail
	Cap	The capacity of the CS
	Rem_{Cap}	Remaining capacity of the CS
	Av	Indicator for availability for charging from CS
	D_c	Number of connected devices
	Cc1	Rate of charging for type 1 charger
	Cc2	Rate of charging for type 2 charger

been given, and Table 4 shows the charging station structure. In order to determine the net energy/power demand subtended at the electric vehicle charging station, the number of vehicles connected to a charging station must be determined along with the mode in which they are being connected. The vehicle can be connected to the charging station either in charging mode or in discharging mode. The vehicle, once connected to the charging station, will not be available for requesting connection to any of the charging stations, hence the availability of EV, i.e. EV_{av} is set to 0 otherwise it is 1. The electric vehicle can draw from or inject power to the grid; the decision of whether the vehicle would be connected in charging or discharging mode would be taken by the electric vehicle owner. The decision of the EV owner would depend on the psychological behaviour of the owner, state of charge (SoC) of the vehicle, and pricing of the electricity. The psychological behaviour of the driver has been modelled using the equation given below:

$$\mathrm{E\ V_{Prob}} = 100\mathrm{SoC}_i - \eta_i \sin\left(\frac{2\pi}{100} \times \mathrm{SoC}_I\right) \tag{10}$$

Here, EV_{Prob} is the probability that the EV owner would request a connection to charging station, η_i is the skewness factor. The SoC and the maximum distance travelled by the vehicle are related to one another [22]. Thus, it can be stated that

$$D = f\,(\mathrm{SoC}) \tag{11}$$

The EV owner would post charging/discharging request to the charging station CS_{id} if distance Cs_d is less than the distance (D) that can be travelled by the EV and slots are available for connecting EV, i.e. ($Cd\ b_i = 1$). The EV agent would have its location information as EV_{loc} along with information of expected time T_{stopa} by which the ongoing trip would be completed. The T_{stopa} is obtained using the following equation:

$$T_{\mathrm{stopa}} = \frac{D}{\mathrm{EV_{Speed}}} \tag{12}$$

$$T_e = T - T_{\mathrm{start}} \tag{13}$$

$$T_r = T_{\mathrm{stop}} - T_e \tag{14}$$

The charging status c_{stat} of the electric vehicle V_{id} is unity if the vehicle is connected to the charging station in-charging mode; otherwise, it is zero. The multiagent representing charging station comprises various parameters given in Table 4. Here, the Cap stands for the capacity of the charging station.

Rem_{Cap} represents the remaining capacity in the charging station. Av is used as an indicator for availability of the charging station is available for accepting the charging/discharging request of the requesting electric vehicle if Av is unity.

The behaviour of EV driving and charging has been modelled extensively by taking the number of vehicles as $N_{vehicle}$ and using β distribution function for representing the transportation network load and traffic. The β-distribution has been discussed as one of the continuous distribution functions that could be used to model the traffic behaviours in [23]. The steps used in agent-based modelling EV have been shown in Figure 6. Here get SoC, and get cs_req are subroutines used to determine the SoC of EV and its charging request status. The β pdf parameters are obtained so as to fit the traffic scenario, the entire duration of 24 h has been segregated into eight segments (A. II), and the alpha and beta parameters are obtained for each of the segments. The beta distribution is used for random polling of traffic scenarios by each EVagent vehicle. It is assumed that the EVs are publicly owned by the state transport corporation. The net power drawn or injected by the EV can be

17521424, 2023, 11, Downloaded from https://ietresearch.onlinelibrary.wiley.com/doi/10.1049/rpg2.12463 by Indian Institute Of Technology, Wiley Online Library on [26/03/2024]. See the Terms and Conditions (https://onlinelibrary.wiley.com/terms-and-conditions) on Wiley Online Library for rules of use; OA articles are governed by the applicable Creative Commons License

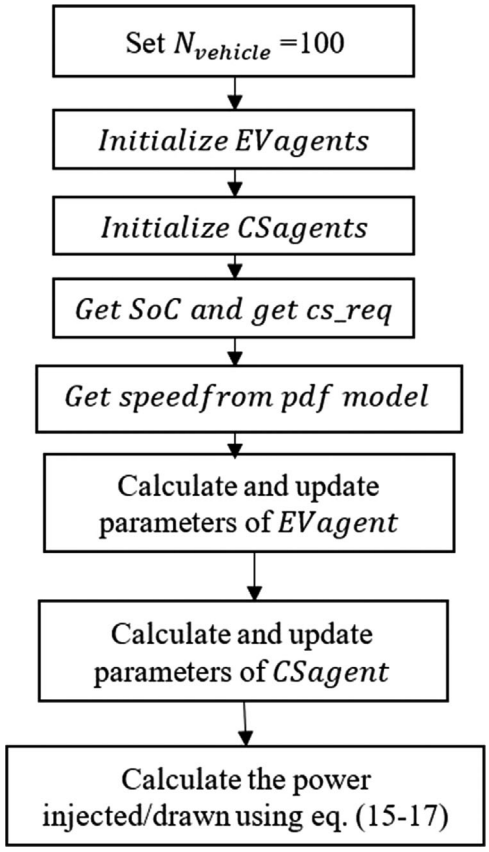

FIGURE 6 Algorithmic steps used in modelling of EV

obtained as

$$E^{\mathrm{EV},i} = P_t^{\mathrm{EV},i} \times \left(t_{\mathrm{start}} - t_{\mathrm{stop}}\right) \tag{15}$$

$$P_t^{\mathrm{EV},i} = \begin{cases} c_t^{r,i} & \text{if charging} \\ -d_t^{r,i} & \text{if discharging} \end{cases} \tag{16}$$

Net power injected/drawn from the grid by the kth Charging Stations could be obtained using the Equation (17).

$$P_k^{\mathrm{CS}} = \sum_{i=1}^{\mathrm{nev}} P_i^{\mathrm{EV}} \tag{17}$$

4.2 | Modelling of DER

The wind and solar PV-based DERs have been modelled using the equivalent average models. The uncertainty modelling has been done using beta distribution for solar-based DER and Weibull distribution for wind-based DERs. Many models have been proposed in the literature for short-term load forecasting that may be utilised for forecasting the load of the impending hours. The predicted wind speed and solar irradiance have been used to obtain the equivalent power produced by the solar or wind DER using Equation (18) or (23).

$$f\ (s_i) = \begin{cases} \dfrac{\tau\ (\alpha_i + \beta_i)}{\tau\ (\alpha)\ \tau\ (\beta_i)} \cdot s_i^{\alpha_i - 1} \cdot (1 - s_i)^{\beta_i - 1} & 0 \le s_i \le 1 \\ \alpha \ge 0; & \\ \beta_i \le 0 & \\ 0 & \text{otherwise} \end{cases} \tag{18}$$

Where, $s_i \in [0, 1]$ stands for the solar irradiance (kW/m^2), $f(s_i)$ represents the probability distribution factor (Beta), with s_i α_i and β_i as the parameters of beta pdf. After modelling solar irradiance, the solar plant output can be modelled as

$$P_i^s = g_s\ \left(s_i, \theta_i^s\right)\ = N_i\ \cdot \mathrm{FF}_i \cdot V_{yi} \cdot I_{yi} \tag{19}$$

$$I_{yi} = s_i\ \cdot \left[I_{sc_i} + k_{c_i}\ (T_{ci} - 25)\right] \tag{20}$$

$$V_{yi} = V_{oc_i}\ - k_{vi} \cdot T_{ci} \tag{21}$$

$$T_{c_i} = T_{\alpha_i}\ + s_i \cdot \frac{N_{ot\,i} - 20}{0.8} \tag{22}$$

Where, P_i^s, $g_s(\cdot)$, θ_i^s, k_{vi},k_{ci} are output power of the ith solar power plant, solar generation function, operational parameter, voltage, and current temperature coefficients, respectively. FF_i is the fill factor, $I_{\mathrm{sc}\,i}$,$V_{\mathrm{oc}\,i}$, V_{MPP_i} represents the short circuit current (A), open-circuit voltage (V), and maximum power point voltage. $N_{\mathrm{oc}\,i}$, T_{ci}, $T_{\alpha i}$ are the normal operating temperature, cell temperature, and ambient temperature, respectively. For wind power plants, the uncertainty in wind speed has been modelled using

$$F\ (v_i)\ = \frac{k_i}{c_i} \left\{\frac{v_i}{c_i}\right\}^{(k_i - 1)} \exp\left[-\left(\frac{v_i}{c_i}^{(k_i - 1)}\right)\right] \tag{23}$$

$$P_i^w = g_w\left(v_i, \theta_i^w\right)$$

$$= \begin{cases} 0 & \\ P_{ri} \cdot \dfrac{v_i - v_{ci}}{v_{ri} - v_{ci}} & v_{ci} \le v_i \le v_{ri} \\ P_{ri} & v_{ri} \le v_i \le v_{coi} \end{cases} \tag{24}$$

Here, k_i, $v_i \ge 0$, c_i are shape index, wind speed, and scale index, respectively. Whereas, θ_i^w, $v_c i$, v_{coi}, v_{ri}, and P_{ri} are the operation parameter, cut-in, cut-out, rated wind speed, and rated power output of ith wind DG.

4.3 | Description of the employed blockchain system

The Ganache-based environment has been used for the simulation of the Ethereum blockchain network. The details of

17521424, 2023, 11, Downloaded from https://ietresearch.onlinelibrary.wiley.com/doi/10.1049/rpg2.12463 by Indian Institute Of Technology, Wiley Online Library on [26/03/2024]. See the Terms and Conditions (https://onlinelibrary.wiley.com/terms-and-conditions) on Wiley Online Library for rules of use; OA articles are governed by the applicable Creative Commons License

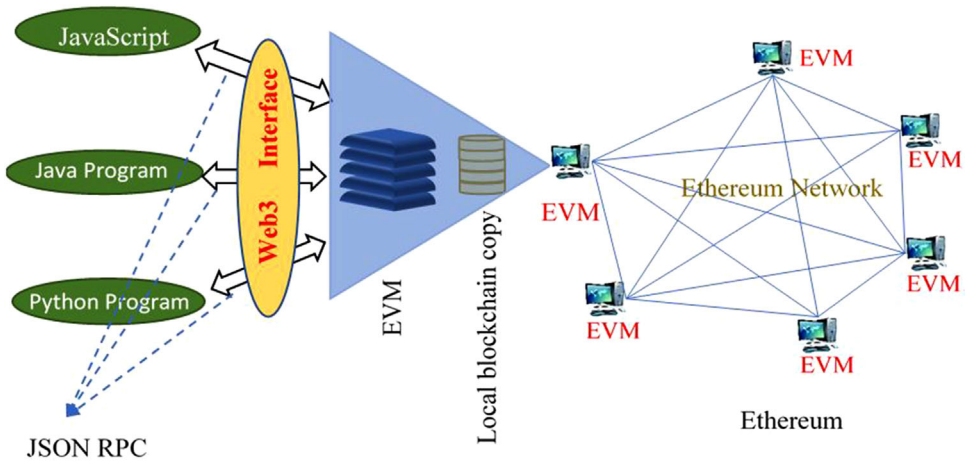

FIGURE 7 Schematic illustration of blockchain implementation through the python interface

blockchain implementation are discussed in this section. The schematic representation of the Ethereum based blockchain implementation has been illustrated in Figure 7. The smart contract deployed in blockchain could be accessed either from the front-end user applications (Ethereum wallets), dedicated front-end applications/web interfaces, or Web3 Interface for developmental purposes. Web3 interface could be exploited for accessing the smart contract deployed on the Ethereum blockchain through the EVM (Ethereum virtual machine) node. The Web3 interface could be used either by Python, JavaScript, or Java programs. For the work under consideration, we have used python language through the Web3.py library to access the blockchain deployed in the Ganache environment at the local-host of the system. The developmental process requires accessing the private and public keys of multiple accounts (of blockchain environment). The transaction would cost money in terms of gas (blockchain unit for transaction charge); therefore, we have used the Ganache simulation environment for the entire developmental process. Figure 8 shows the Ganache environment that has been used for developing and testing Ethereum based blockchain smart contracts. The smart contracts are created using Solidity. Solidity is a language used for creating smart contracts for the Ethereum blockchain. The interaction between various components of the smart grid is shown in Figure 2.

The participants, namely the LA (Local Aggregators), EV owners, electric vehicle charging stations (EVCS), DER's, grid, would exchange their bids to the blockchain. The information of settled transactions is acquired by the command-and-control centre and communicated to the DSO. The DSO validates the transaction and obtains the optimal settings of the devices for the settled transaction.

5 | PROBLEM FORMULATION OF DSO

The overall problem of analysing the effect of blockchain-based energy transaction on ADN has been framed as a multistage problem. The first stage of the problem deals with loss minimisation, and the second is the ADC evaluation. At first, the various parameters in ADN are set to minimise the overall losses in the transactions scheduled and settled through the blockchain-based mechanism. Once the control parameters are determined, the ADC for the system is calculated. Thus, the overall evaluation process is a two-stage process involving the determination of the control parameters so as to minimise the losses for the settled and scheduled transactions over the blockchain at the first stage and then obtain the ADC of the system by solving the Equation (33) at the second stage.

5.1 | Loss minimisation

The information pertaining to the forecasted/estimated generation/load at each node of ADN would be acquired by the DSO. The DSO would determine the optimal control settings for meeting the desired operational objectives. In the proposed method, the DSO aimed at minimising the overall losses of the ADN. This has been achieved by minimising the objective function given in equation

$$\text{Min}\left(\mathcal{L}(t)\% = \sum_{i=0}^{n-1} \% r_i \frac{P_{i,t}^2 + Q_{i,t}^2}{V_{i,t}^2}\right) \tag{25}$$

In Equation (25) $\mathcal{L}(t)$ is the total loss of the ADN at time t. $P_{i,t}$, $Q_{i,t}$ and $V_{i,t}$ are active power, reactive power and voltage at ith bus respectively whereas r_i is the resistance between ith and ith $-$ 1 bus, n is the total number of branches. The parameters to be controlled in the ADN includes the tap settings of OLTC, number of the capacitor bank, and voltage regulators deployed in the distribution network. The objective of Equation (25) is achieved by the DSO while adhering to the underlying equality and inequality constraints.

17521424, 2023, 11, Downloaded from https://ietresearch.onlinelibrary.wiley.com/doi/10.1049/rpg2.12463 by Indian Institute Of Technology, Wiley Online Library on [26/03/2024]. See the Terms and Conditions (https://onlinelibrary.wiley.com/terms-and-conditions) on Wiley Online Library for rules of use; OA articles are governed by the applicable Creative Commons License

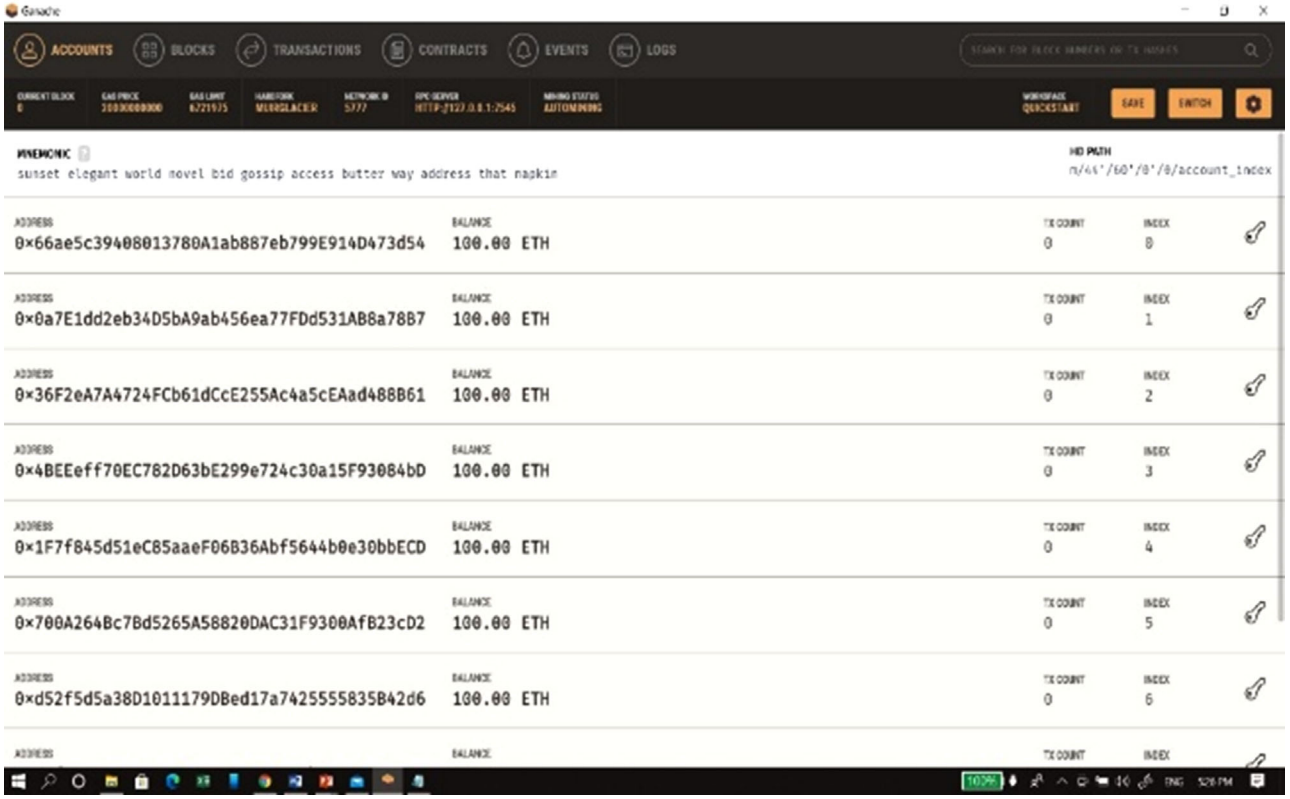

FIGURE 8 Ganache interface

5.1.1 | Equality constraints

$$P^{\text{source}} + P^{\text{S}} + P^{\text{W}} \pm P^{\text{CS}} - P^{\text{load}} - P^{\text{loss}} = 0 \quad (26)$$

Here, P^{W} and P^{S} represents the total wind and solar power fed into the ADN, P^{load}, P^{loss} are the total load, and total losses of the *ADN* while P^{CS} is the total power drawn by the charging stations. These values are expressed in the equations

$$\%P^{\text{S}} = \sum_{i=1}^{\text{ns}} \%P_i^{\text{s}}; \%\%P^{\text{W}} = \sum_{j=1}^{\text{nw}} \%P_j^{\text{W}} \quad (27)$$

$$\%P^{\text{CS}} = \sum_{k=1}^{\text{ncs}} \%P_k^{\text{CS}}; \%\%P^{\text{load}} = \sum_{m=1}^{\text{nl}} \%P_m^{\text{load}} \quad (28)$$

$$\%P_{\text{loss}} = \sum_{i=0}^{n-1} \%r_i \frac{P_{i,t}^2 + Q_{i,t}^2}{V_{i,t}^2} \quad (29)$$

5.1.2 | Inequality constraints

$$P_{i,j}^{\min} \le P_{i,j} \le P_{i,j}^{\max} \quad (30)$$

$$Q_{i,j}^{\min} \le Q_{i,j} \le Q_{i,j}^{\max} \quad (31)$$

$$V_i^{\min} \le V_i \le V_i^{\max} \quad (32)$$

5.2 | ADC evaluation

The ADC expressed by Equation (7) could be defined as a maximisation problem given as Equation (33).

$$\text{Max}\lambda \quad (33)$$

$$\text{where}: \%\lambda\% = \sum_{i=1}^{nl} \%Pd_i - \sum_{i\%=\%1}^{nl} Pd_0 \quad (34)$$

$$\text{s.to}: -P^{\text{source,min}} \le P^{\text{source}} \le P^{\text{source,max}} \quad (35)$$

Along with the constraint mentioned in Equation (35), the power flow constraints are also to be ascertained.

5.3 | Blockchain efficiency factor (BC_{ef})

In order to assess the impact of energy trading over blockchain and its impact on the ADN a novel index BC_{ef} have been

17521424, 2023, 11, Downloaded from https://ietresearch.onlinelibrary.wiley.com/doi/10.1049/rpg2.12463 by Indian Institute Of Technology, Wiley Online Library on [26/03/2024]. See the Terms and Conditions (https://onlinelibrary.wiley.com/terms-and-conditions) on Wiley Online Library for rules of use; OA articles are governed by the applicable Creative Commons License

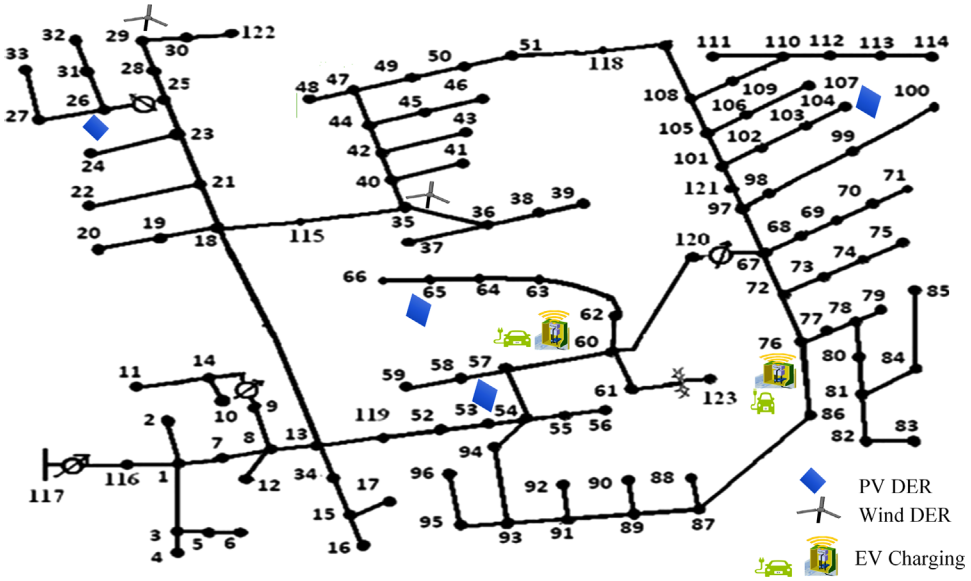

FIGURE 9 Test system: modified IEEE 123 bus feeder

proposed in this article. The index BC_{ef} could be mathematically defined as

$$B\ C_{ef}=\frac{TEP}{TELMCP+TELMP} \tag{36}$$

Here,

TEP = Total energy sold × price (for base case)
TELMCP = Total energy sold at LMCP × LMCP (when blockchain-based energy transaction is considered).
TELMP = Total energy sold at LMP × LMP (under blockchain energy transaction).

When the blockchain-based energy transaction is considered, then the following cases may be seen:-

(i) LMCP < LMP

In this case, the LMCP is considered for bid settlement till the localised market clearing volume. Beyond the LMCV, the energy is sold at the LMP.

(ii) LMCP > LMP

In this case, the clearing price would be set as LMP, and the entire buying bid would be settled at this price.

The factor BC_{ef} represents the extent to which the blockchain-based energy transaction affects the grid operation in terms of economies and losses. If the value is unity, then there is no effect of incorporating blockchain-based energy transactions. In essence, the blockchain efficiency factor, i.e. BC_{ef} has been propounded by the authors as an index to assess the impact of blockchain-based energy transactions on ALP, ADC, LM, and losses of the ADN. The BC_{ef} values greater than unity indicates that deployed blockchain-based energy transaction has a positive effect on the system, while values less than unity indicates that deploying blockchain-based energy transaction would not be economical. The higher values of BC_{ef} indicates greater impact of blockchain-based transactions on the grid. For the case when the value is unity, there would be no effect of deploying the blockchain-based energy transaction. In the results for the base case, the BC_{ef} is unity as blockchain has not been considered.

5.4 | Solution methodology

Pattern Search (PS) based optimisation technique has been used for solving the objective functions expressed by Equations (25) and (33). The application of PS for ATC assessment and enhancement at the transmission level has been investigated in ref. [24]. Being a direct search algorithm, in PS, information pertaining to the gradient of the objective function is not required. Direct search algorithm searches a set of points around the current point, looking for the optimum point of the problem.

6 | RESULT ANALYSIS AND DISCUSSION

The proposed method of this paper has been utilised for testing on the modified IEEE 123 bus test system as inked in Figure 9. Modification to the test system has been done by incorporating

(i) public charging stations of 200 kW capacity at nodes 60 and 76,

17521424, 2023, 11, Downloaded from https://ietresearch.onlinelibrary.wiley.com/doi/10.1049/rpg2.12463 by Indian Institute Of Technology, Wiley Online Library on [26/03/2024]. See the Terms and Conditions (https://onlinelibrary.wiley.com/terms-and-conditions) on Wiley Online Library for rules of use; OA articles are governed by the applicable Creative Commons License

TABLE 5 Various cases considered for the analysis

S.N	Component	Case 1	Case 2	Case 3	Case 4
1	PV	×	✓	✓	✓
2	WIND	×	✓	✓	✓
3	EV	×	×	✓	✓
4	MG	×	×	×	✓

(ii) at nodes 35 and 29, two wind DER have 800 kW, and 700 kW ratings have been placed.
(iii) nodes 26, 100, 65, and 54 are provided, with PV DER having ratings of 400, 100, 400, and 400 kW each.

The system has been analysed for four different cases; details of various cases can be found in Table 5. Namely, four different cases have been considered depending upon the consideration of PV, WIND, EV, and micro-grid (MG). For the base case, i.e. 'Case 1', energy trading via blockchain has not been considered. On the contrary, blockchain-based energy trading has been considered for all the other cases. The behaviour of various components of ADN during the 24 h of simulation and the effect on various parameters have been discussed in the following section:

a. The behaviour of Charging stations

The power demand subtended by CS1 and CS2 considered in test system during simulation of 24 h has been shown in Figure 10. The results are obtained using the agent-based EV behaviour simulation discussed in Section 4.1. It can be observed from the plots that the power subtended by the two charging stations on the ADN varies with time of day. During simulation N_{vehicle} has been taken as 100 and load demand instants (at resolution of 15 min) are provided by the EV agent while analysis of the present system.

b. DER deviation from forecasted value

The deviations in power produced by the DERs would eventually have economic effects. The deviations in the wind and PV DER considered during the simulation have been shown in Figure 11(a,b).

It can be seen from the results that in the base case, the deviations are zero because in the base case, the ADN has not been considered. In other cases where the ADN has been considered there seems to be deviations in both PV and wind DER. These deviations would have an economic impact on the overall system; therefore, adequate forecasting of DER is essential. These deviations represent the difference between the forecasted and actual power at a particular time instant. These plots are significant as this highlight the uncertainty and degree of variability being introduced into the grid from the ADN.

c. Market indicators (LMCP and BC_{ef})

The plots of LMCP and BC_{ef} have been given in Figures 12 and 13. It could be observed from Figure 13 that the BC_{ef} for case 1 is 1, as block-chain based energy transaction has not been considered during the base case simulation. The factor BC_{ef} as seen from the plot for other cases can vary from one-time instant to another time instant, the effect of block chain becomes more and more dominant when the active devices in the system increase. Higher the deviation of BC_{ef} from unity, higher would be the impact of considering the blockchain based energy transaction on ADN.

The LMCP determination for the considered test system has been shown for a typical case in Figure 5. Here the intersection points of the seller's and buyer's bid amount are taken as the LMCP. In the plot, the LMCP value is 3.8, and LMCV (localised marginal clearing volume) is 1800 kW. Further, in Figure 12, the market-clearing price of ADN under various

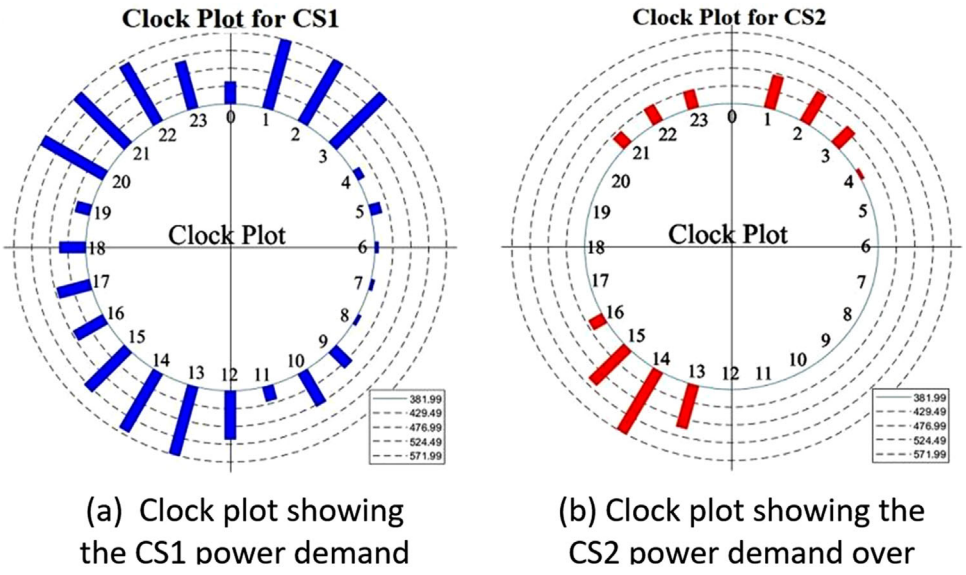

(a) Clock plot showing the CS1 power demand

(b) Clock plot showing the CS2 power demand over

FIGURE 10 Clock plot showing the CS2 power demand over 24 h

17521424, 2023, 11, Downloaded from https://ietresearch.onlinelibrary.wiley.com/doi/10.1049/rpg2.12463 by Indian Institute Of Technology, Wiley Online Library on [26/03/2024]. See the Terms and Conditions (https://onlinelibrary.wiley.com/terms-and-conditions) on Wiley Online Library for rules of use; OA articles are governed by the applicable Creative Commons License

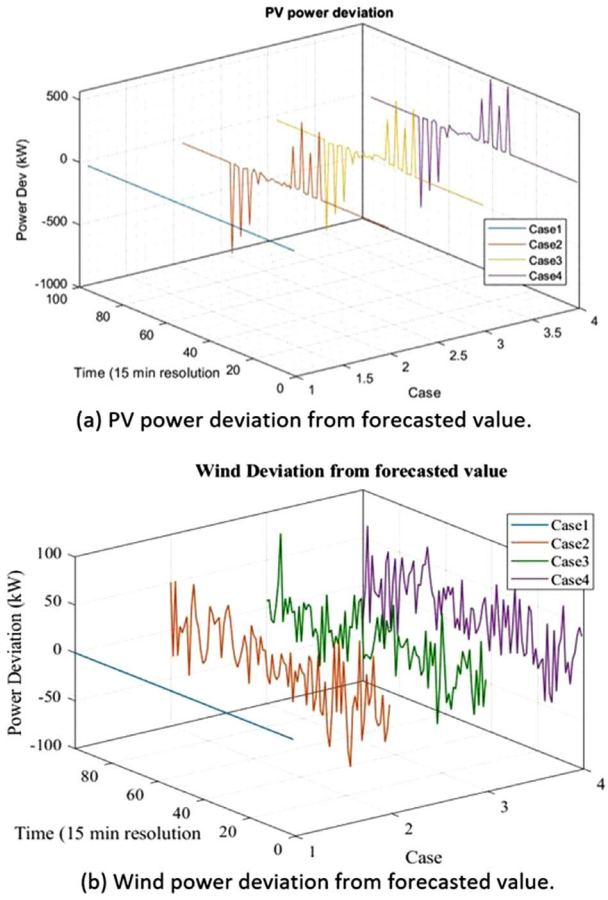

FIGURE 11 Deviation in power produced by DER's in ADN at resolution of 15 min for 24 h. a) PV power deviation from forecasted value. b) Wind power deviation from forecasted value

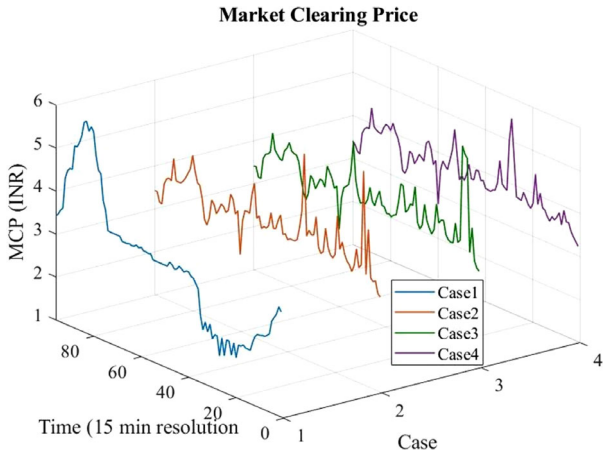

FIGURE 12 LMCP of ADN at resolution of 15 min for 24 h

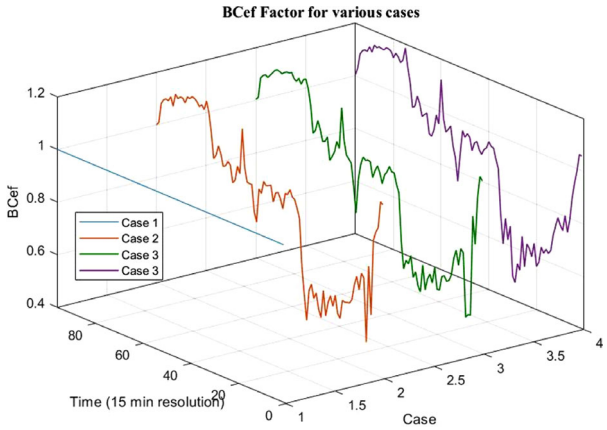

FIGURE 13 Blockchain-based efficiency factor

cases is shown. The plot for case 1 (i.e. base case) represents LMP (locational marginal price) subtended at the DSS for the considered test system. The market data of Gujarat (practical Indian data) have been considered for the analysis purpose. The bid and actual values of various components of ADN have been inked in Table 6. In this table, the bid value of the component is the bid submitted at $(t-1)$th instant (t being the current instant). The actual value is the actual power sold or purchased to/from the grid. The actual price represents the

TABLE 6 Bid and actual value of power (kW) and price (INR/kW)

		Time				Time			
		10:00 AM				12:00 PM			
		Bid		Actual		Bid		Actual	
SN	Component	Power	Price	Power	Price	Power	Price	Power	Price
1	PV 1	48.3682	5.9	47.3513	3.63	97.222	5.96	95.2177	3.77
2	PV 2	191.348	5.974	189.4047	3.63	387.9903	5.974	380.8725	3.77
3	PV 3	193.8066	5.89	189.4043	3.63	384.5391	5.9152	380.8744	3.77
4	PV 4	468.6877	2.44	466.2471	3.63	923.7549	2.51	929.1471	3.77
2	WIND 1	834.6963	3.784	816.0642	3.63	558.073	3.784	540.9797	3.77
3	WIND 2	342.2129	6.15	327.3964	3.63	223.3798	6.3	219.8758	3.77
3	EV	170.254	4.8595	170	3.63	147.4016	5.1332	150	3.77
4	MG	33.2089	7.052	30	3.63	59.4385	7.167	60	3.77

17521424, 2023, 11, Downloaded from https://ietresearch.onlinelibrary.wiley.com/doi/10.1049/rpg2.12463 by Indian Institute Of Technology, Wiley Online Library on [26/03/2024]. See the Terms and Conditions (https://onlinelibrary.wiley.com/terms-and-conditions) on Wiley Online Library for rules of use; OA articles are governed by the applicable Creative Commons License

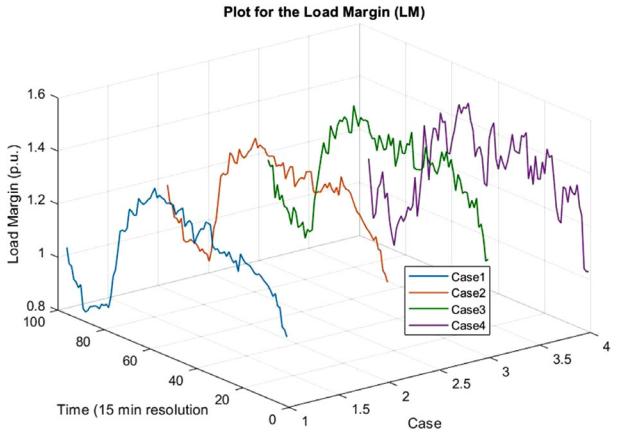

FIGURE 14 Load margin plot for various cases of modified IEEE 123 bus test system

LMCP determined at and used for clearing/settling the transactions. The actual power withdrawal/injected by each peer is communicated to the blockchain at the address of the smart contract from which the financial settlements could be materialised without the necessity of third-party mediation. The effect of blockchain based energy transactions would become more and more prominent as the activeness of the active distribution network increases. The activeness of the active distribution network represents the degree of DER penetration, presence of EV charging stations, and extent of actively participating prosumer nodes. The limitation of blockchain based energy transactions lies in the fact that energy required for maintaining and scaling up the blockchain based system would be very high (6).

d. Aggregated load profile, loadability margin, and available distribution capability

The Load Margin plot for various cases of modified IEEE 123 bus test system under study has been shown in Figure 14. The result of Figures 15 and 16 indicates the variation in available distribution capability and aggregated load profile of the system with the help of a 3D bar graph. The plots have different cases on the first axis, time on the second axis, and the magnitude of the quantity being represented on the third axis. The time axis has been shown for 4 h in each subplot, as the time interval for bidding and energy scheduling is taken as an interval of 15 min. Therefore the number of time instants indicated on the time axis is 16 (i.e. 4×4, since 1 h would have four instants of 15 min).

It can be observed that the LM depends on the time of day as well as the activeness of the various energy vendors in the market, and hence the blockchain-based energy transaction affects the LM of the overall system. The ADC variation for the considered test system is shown in Figure 15. The results are shown corresponding to all four cases at a

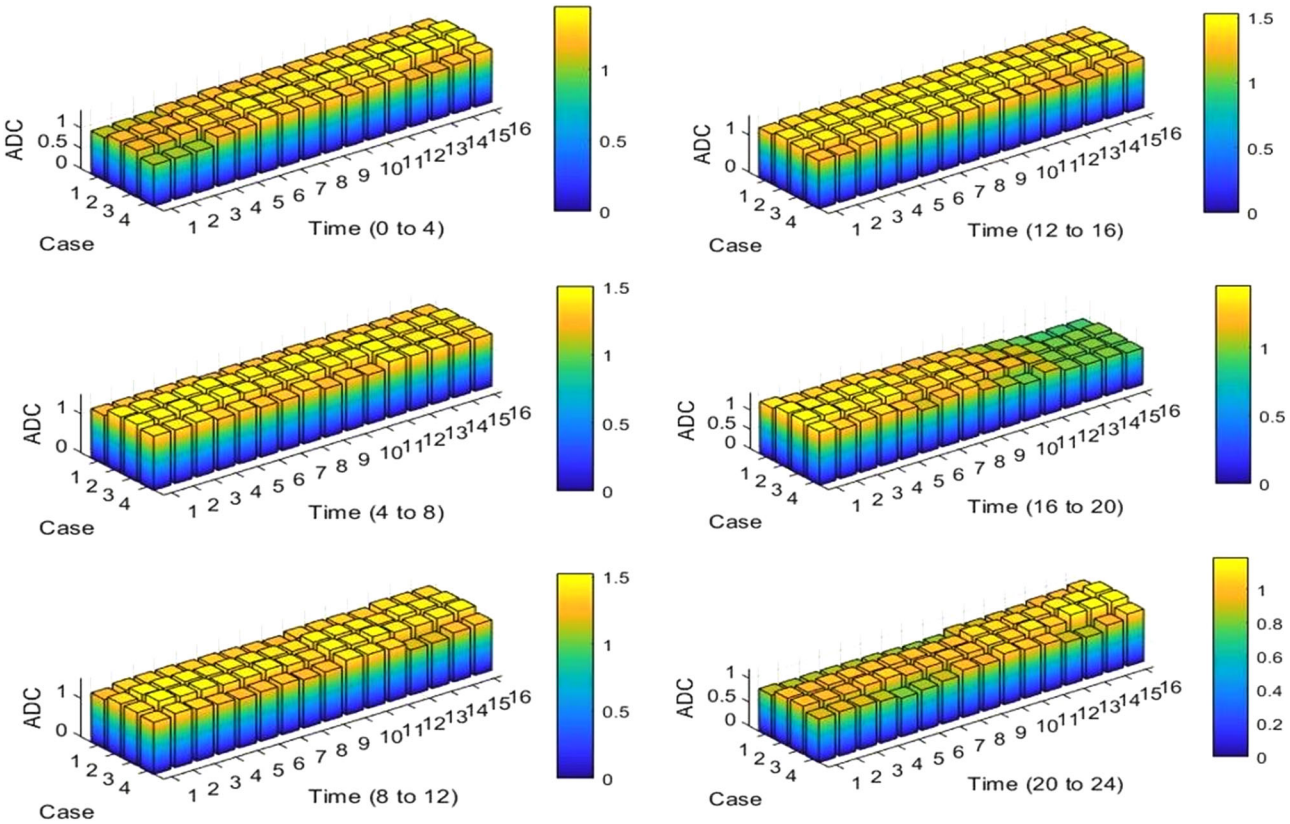

FIGURE 15 ADC of ADN at resolution of 15 min for 24 h

17521424, 2023, 11, Downloaded from https://ietresearch.onlinelibrary.wiley.com/doi/10.1049/rpg2.12463 by Indian Institute Of Technology, Wiley Online Library on [26/03/2024]. See the Terms and Conditions (https://onlinelibrary.wiley.com/terms-and-conditions) on Wiley Online Library for rules of use; OA articles are governed by the applicable Creative Commons License

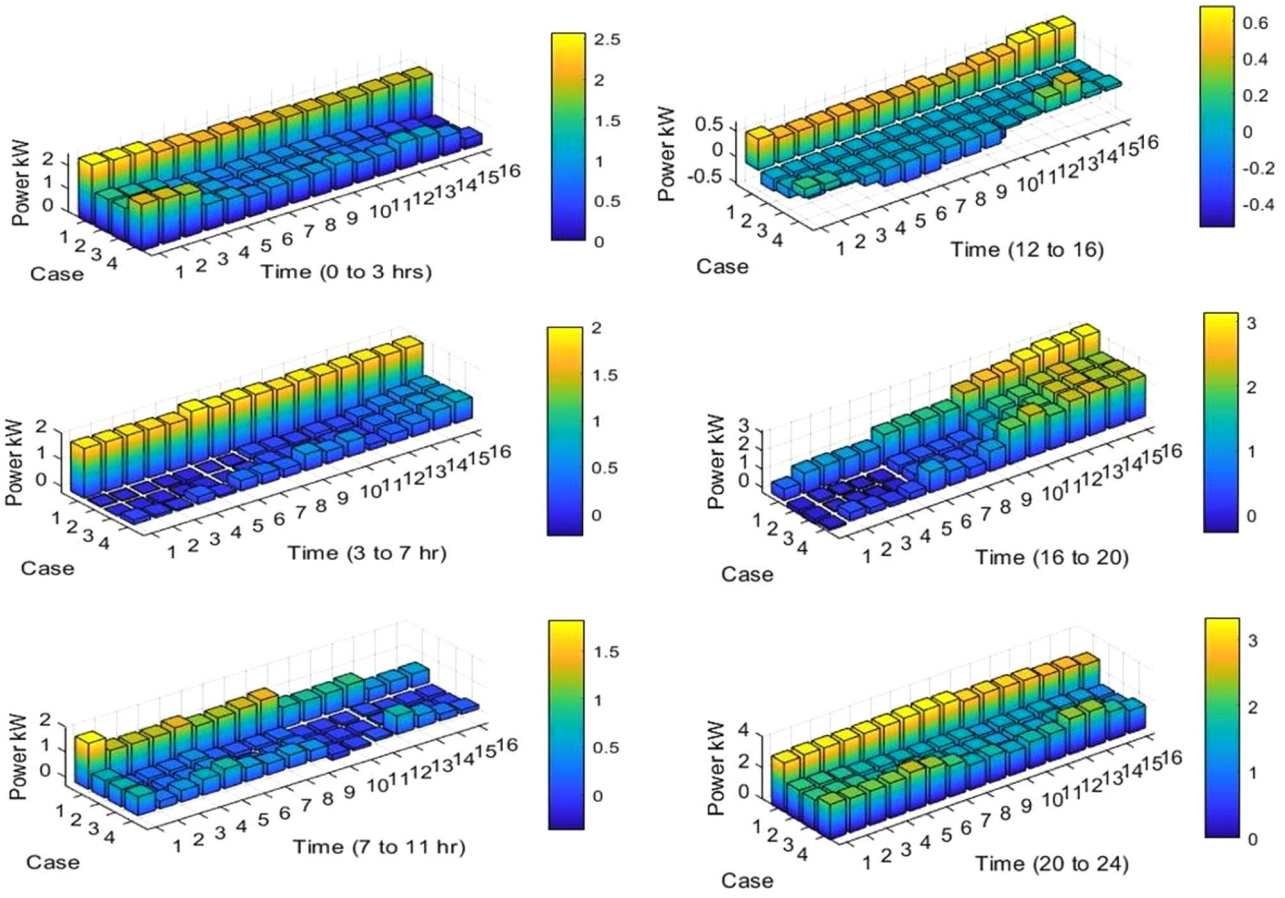

FIGURE 16 Aggregated load profile of ADN at resolution of 15 min for 24 h

resolution of 15 min for the duration of 24 h. The result has been shown in terms of bar plot, and each subplot contains the plot for 4 h duration. It can be observed from the figure that the ADC of the ADN depends on the time of the day. We can also observe from the plot shown in Figure 15 that ADC is distinct for all the cases under consideration (i.e. case1, case2, case3, and case4). The distinct ADC values can be attributed to different values of ALP of the system for different cases, as inked in Figure 16. The aggregated load subtended by the ADN at the interface of the transmission and distribution system also gets affected due to the presence of DERs and energy trading through the block-chain based mechanism. This can be inferred from the various subplots shown the Figure 16. It can be observed from the subplot for time duration 12 to 16 p.m. that at some time instants, the ALP is negative. These represent the instants at which the total generation of the ADN surpassed its load and is feeding power back to the grid. The ADC information would be vital in the techno-economic operation of ADN when multiple and probably mobile sources/sinks of electric power (i.e. EV) are being integrated more and more into the ADN grid. It is imperative to mention that the effect of incorporation of the EV would become more dominant if the number of EVs used in the simulation process is increased.

7 | CONCLUSION

The effect of distributed energy resources and their participation in energy trading over a blockchain-based framework has been analysed. The impact has been investigated primarily on the available distribution capability, aggregated load profile, and load ability limit of the active distribution network. The concept of localised market clearing price and localised market clearing volume has been introduced, and the methodology for its determination is discussed. An index BC_{ef} for quantifying the impact of blockchain-based energy trading have been proposed. The technique presented has been applied to the modified IEEE 123 bus distribution system. It could be inferred from the results obtained during the simulations that employing a blockchain for energy transactions would have a considerable effect on ALP, ADC, LM, and losses of the ADN. Thus, if appropriately utilised, the blockchain-based system could help in efficiently managing both economic and operational aspects of the ADN.

NOTATION

$\mathcal{S}_i(\cdot), \mathcal{B}_i(\cdot)$	Seller and buyer bid functions
$\beta_i, \psi_i, \gamma_i$	Are bid coefficient of ith unit
ADC	Available distribution capability

17521424, 2023, 11, Downloaded from https://ietresearch.onlinelibrary.wiley.com/doi/10.1049/rpg2.12463 by Indian Institute Of Technology, Wiley Online Library on [26/03/2024]. See the Terms and Conditions (https://onlinelibrary.wiley.com/terms-and-conditions) on Wiley Online Library for rules of use; OA articles are governed by the applicable Creative Commons License

ADN	Active distribution network
ALP	Aggregated load profile
DER	Distributed energy resources
DLMP	Distribution locational marginal pricing
DN	Distribution network
DSO	Distribution system optimiser
DSS	Distribution system substation
EDC	Existing distribution commitments
EV	Electric vehicle
EVCS	Electric vehicle charging station
EVM	Ethereum virtual machine
HEV	Hybrid electric vehicle
LA	Local aggregator
LMCP	Localised marginal clearing price
LMCV	Localised marginal clearing volume
LMP	Locational marginal pricing
TDC	Total distribution capability
TN	Transmission network
VPP	Virtual power plant
AL_t	Aggregated load at time t
BC_{ef}	Blockchain efficiency factor
$DRes$	Distribution reserves
$Pd_{i,t}$	Buying bid of ith purchaser at time t.
$Pg_{i,t}$	Selling generation bid of ith seller at time t.
$\mathcal{IC}_i$	Installation cost of ith generation unit.
$\mathcal{OM}_i$	Operation and maintenance cost of ith generation unit.

CONFLICT OF INTEREST

The author and any co-authors have no conflict of interest to disclose.

ORCID

Devesh Shukla https://orcid.org/0000-0003-4851-6615

REFERENCES

1. Shukla D., Singh S.P.: Aggregated effect of active distribution system on available transfer capability using multi-agent system based ITD framework. IEEE Syst. J. 15(1), 1401–1412 (2020)
2. Shukla D., Singh S., Singh S.P., Thakur A.K., Singh S.P.: Block-chain based energy trading in ADN with its probable impact on aggregated load profile and available distribution capability. In: *2020 2nd International Conference on Smart Power Internet Energy Systems (SPIES)*, pp.486–491. IEEE, Piscataway, NJ (2020)
3. Lin Y., Yang M., Wan C., Wang J., Song Y.: A multi-model combination approach for probabilistic wind power forecasting. IEEE Trans. Sustainable Energy 10(1), 226–237, (2019)
4. Yang X., Zhang Y., Yang Y., Lv W.: Deterministic and probabilistic wind power forecasting based on bi-level convolutional neural network and particle swarm optimization. Appl. Sci. 9(9), 1794 (2019)
5. Abuella M., Chowdhury B.: Solar power probabilistic forecasting by using multiple linear regression analysis. In: *SoutheastCon 2015*, pp. 1–5. IEEE, Piscataway, NJ (2015)
6. Olama M., Melin A., Dong J., Djouadi S., Zhang Y.: Stochastic short-term high-resolution prediction of solar irradiance and photovoltaic power output. In: *2017 North American Power Symposium (NAPS)*, pp. 1–6. IEEE, Piscataway, NJ (2017)
7. Ehsan A., Yang Q.: Active distribution system reinforcement planning with EV charging stations-part I: uncertainty modelling and problem formulation. IEEE Trans. Sustainable Energy 11(2), 970–978 (2019)
8. Esmat A., de Vos M., Ghiassi-Farrokhfal Y., Palensky P., Epema D.: A novel decentralized platform for peer-to-peer energy trading market with blockchain technology. Appl. Energy 282(A), 116123, (2021)
9. Doan H.T., Cho J., Kim D.: Peer-to-peer energy trading in smart grid through blockchain: a double auction-based game theoretic approach. IEEE Access 9, 49206–49218, (2021)
10. Hosseinnezhad V., Hayes B., O'Regan B., Siano P.: Practical insights to design a blockchain-based energy trading platform. IEEE Access 9, 154827–154844 (2021)
11. Yang J., Paudel A., Gooi H.B.: Compensation for power loss by a proof-of-stake consortium blockchain microgrid. IEEE Trans. Ind. Inf. 17(5), 3253–3262 (2021)
12. Alashery M.K., et al.: A blockchain-enabled multi-settlement quasi-ideal peer-to-peer trading framework. 12(1), 885–896 (2021)
13. Abdella J., Tari Z., Anwar A., Mahmood A., Han F.: An architecture and performance evaluation of blockchain-based peer-to-peer energy trading. IEEE Trans. Smart Grid 12(4), 3364–3378, (2021)
14. Di Silvestre M.L., Gallo P., Ippolito M.G., Sanseverino E.R., Zizzo G.: A technical approach to the energy blockchain in microgrids. IEEE Trans. Ind. Inf. 14(11), 4792–4803 (2018)
15. Sharma V.: An energy-efficient transaction model for the blockchain-enabled internet of vehicles (IoV). IEEE Commun. Lett. 23(2), 246–249, (2019)
16. Thakur S., Breslin J.G.: Peer to peer energy trade among microgrids using blockchain based distributed coalition formation method. Technol. Econ. Smart Grids Sustainable Energy 3(1), 5 (2018)
17. Kang J., Yu R., Huang X., Maharjan S., Zhang Y., Hossain E.: Enabling localized peer-to-peer electricity trading among plug-in hybrid electric vehicles using consortium blockchains. IEEE Trans. Ind. Inf. 13(6), 3154–3164, (2017)
18. Liu Z., et al.: A survey on blockchain: a game theoretical perspective. IEEE Access 7, 47615–47643, (2019)
19. Di Silvestre M.L., et al.: Ancillary services in the energy blockchain for microgrids. IEEE Trans. Ind. Appl. 55(6), 7310–7319 (2019)
20. Nakamoto S.: Bitcoin: a peer-to-peer electronic cash system. (2009). https://www.ussc.gov/sites/default/files/pdf/training/annual-national-trainingseminar/2018/Emerging_Tech_Bitcoin_Crypto.pdf, Online accessed, 5 April 2020
21. Gilbert H., Handschuh H.: Security analysis of SHA-256 and sisters. In: Selected Areas in Cryptography, pp. 175–193. Springer, Berlin, Heidelberg (2004)
22. Shekhar A., Prasanth V., Bauer P., Bolech M.: Generic methodology for driving range estimation of electric vehicle with on-road charging. In: *2015 IEEE Transportation Electrification Conference and Expo (ITEC)*, pp. 1–8, IEEE, Piscataway, NJ (2015)
23. Maghrour Zefreh M., Török Á.: Distribution of traffic speed in different traffic conditions: an empirical study in Budapest. Transport 35(1), 68–86 (2020)
24. Shukla D., Singh S.P., Thakur A.K., Mohanty S.R.: ATC assessment and enhancement of integrated transmission and distribution system considering the impact of active distribution network. IET Renew. Power Gener. 14(9), 1571–1583 (2020)
25. IEEE, 1992, IEEE Test Feeders (1992), https://cmte.ieee.org/pes-testfeeders/resources/. Online accessed, 5 April 2020

How to cite this article: Shukla, D., Singh, S., Singh, S.P., Thakur, A.K., Singh, S.P.: Blockchain based energy trading in ADN with its probable impact on aggregated load profile, available distribution capability and loadability margin. IET Renew. Power Gener. 17, 2853–2868 (2023). https://doi.org/10.1049/rpg2.12463

17521424, 2023, 11, Downloaded from https://ietresearch.onlinelibrary.wiley.com/doi/10.1049/rpg2.12463 by Indian Institute Of Technology, Wiley Online Library on [26/03/2024]. See the Terms and Conditions (https://onlinelibrary.wiley.com/terms-and-conditions) on Wiley Online Library for rules of use; OA articles are governed by the applicable Creative Commons License

APPENDIX

A.1. Description of DERs considered in ADN

S. N	Bus	Type	Phases	Rating	Location	PF
1	29	WIND	3	800 *kW*	Node 35	1
2	35	WIND	3	700 *kW*	Node 29	1
3	104	PV	1	400 *kVA*	Node 26	0 to 0.9676
4	26	PV	3	100 *kVA*	Node 100	0 to 0.9676
5	65	PV	3	400 *kVA*	Node 65	0 to 0.9676
6	53	PV	3	400 *kVA*	Node 54	0 to 0.9676

A.2. The parameters of EV and EVCS are used in the simulation

S. N	EV parameter	Value		EVCS Parameter	Value
1	Number of vehicles	100		No of EVCS	2
2	Types of vehicles	Public transport (3 to 30 Kw)		Rating of each station	200 KW capacity Level 1 and level 2 charger
3	SoC Min	20 %		Location of EVCS	Node 60 and 76
4	Vehicle in operation at 0:00 h	10 % of total vehicles			
5	Parameters of β-distribution used for modelling the traffic	Time Instant	α, β		
		0 to 24	2,4		
		24 to 32	3,4		
		32 to 40	4,2		
		40 to 52	4,3		
		52 to 68	3,4		
		68 to 76	4,2		
		76 to 84	3,4		
		84 to 96	2,4		

17521424, 2023, 11, Downloaded from https://ietresearch.onlinelibrary.wiley.com/doi/10.1049/rpg2.12463 by Indian Institute Of Technology, Wiley Online Library on [26/03/2024]. See the Terms and Conditions (https://onlinelibrary.wiley.com/terms-and-conditions) on Wiley Online Library for rules of use; OA articles are governed by the applicable Creative Commons License